Progress In Electromagnetics Research, PIER 104, 183–199, 2010

CO-FREQUENCY INTERFERENCE SUPPRESSION ALGORITHM VIA MAXIMUM SIGNAL MINUS INTERFERENCE LEVEL

L. Kong and M. Luo

School of Electronic Engineering
University of Electronic Science and Technology of China
No. 2006, Xiyuan Avenue, West Hi-Tech Zone, Chengdu, China

Abstract—Co-frequency interference problem is severe in shared-spectrum multistatic radar system, leading to detection problems in applications. In order to mitigate the co-frequency interferences, an adaptive pulse compression algorithm based on Maximum Signal Minus Interference Level criterion (MSMIL) is proposed in this paper, the main idea of which is to adaptively design an appropriate filter at each range cell, maximizing the result of signal power minus interference power, so that both range sidelobes and cross-correlation interference can be suppressed. Simulation results show that the algorithm outperforms the traditional multistatic adaptive pulse compression (MAPC) method in interference suppression. Compared with MAPC method, after one iteration step, the output SIR of the proposed algorithm is increased by about 10 dB. And after two iteration steps, it is increased by more than 40 dB. Moreover, it also outperforms the MAPC in convergence speed.

1. INTRODUCTION

Radio Frequency (RF) spectrum is becoming more and more crowded. In order to maximize the efficient use of RF spectrum, the International Telecommunications Union (ITU) authorizes to share spectrum [1], so the Federal Communications Commission (FCC) and the National Telecommunications and Information Administration (NTIA) share spectrum managements with each other, and the spectrum sharing technologies are studied widely in [2, 3]. These promote the development of shared-spectrum multistatic radar technology.

In shared-spectrum multistatic radar, multiple radars operate in the same spectrum, in close proximity and at the same time,

Corresponding author: L. Kong (uestc.kong@gmail.com).

which is realized by waveform diversity avoiding RF fractricide, thus the efficiency of spectrum is improved. The benefits obtained from shared-spectrum radar system are more information extracted, more efficient spectrum utilization, greater area coverage with shorter revisit time and greater instantaneous bandwidths due to the reduction of spectrum crowding. Typical multistatic radar systems are comprised of only a single transmitter and multiple passive receivers, or employ a different portion of frequency spectrum, while shared-spectrum radars operate in the same frequency band [4, 5]. Although multiple-input multiple-output (MIMO) radar and shared-spectrum radar both are multistatic and transmit orthogonal waveforms [6], all individual radars making up a MIMO radar system work together as a unit to achieve a common goal which generally employs spectral diversity [7]. In contrast, the present work is to enable multiple radars to operate quasi-independently in the same spectrum without interfering with one another. Because radar operates in the same spectrum, where signal and interference occupy the same frequency band, it is impossible to eliminate the interference in the frequency domain similar to other multistatic radar system [8, 9], and the matched filter is not optimal any more in such a situation. Thus, it is crucial to find advanced approaches to mitigate the effect of interference in shared-spectrum multistatic radar.

Blunt and Karl have proposed a multistatic adaptive pulse compression (MAPC) combined with a nonadaptive beamformer to suppress range sidelobes and mutual interference effectively [10]. In [11, 12], MAPC combined with an adaptive beamformer is adopted to obtain better performance, and in [13, 14], a generalized framework is presented to take account of all the potential interferences, including transmit-mainbeam reflected into receive-mainbeam, transmit-mainbeam reflected into receive-sidelobe, transmit-sidelobe reflected into receive-mainbeam, transmit-sidelobe reflected into receive-sidelobe and noise. In general, the MAPC outperforms the matched filter and Least-Squares. However, the adaptive degrees of-freedom of MAPC limit its capability for interference suppression. To circumvent the drawbacks, the hybrid MAPC and CLEAN algorithm has been presented, which provides significant sensitivity improvement over MAPC [15, 16]. All of the MAPC algorithms mentioned above are based on minimizing the mean square error (MMSE) between the desired signal and pulse compression output minimum, and has been limited for the range sidelobes, mutual interference and noise which are considered as a whole.

In this paper, unlike the traditional MAPC algorithms, returned signal echo is constructed as the summation of the target echo caused

by the mainlobe, the target echo caused by the range sidelobes, co-frequency interference from other radars and noise. According to this model, a multistatic adaptive pulse compression technology based on reiterative MSMIL criterion is developed which is denoted as RMSMI. Therefore the reiterative filter is obtained by maximizing the result of signal power minus interference power after pulse compression. Based on the framework, the performance of RMSMI algorithm is manifested by comparing it with that of MAPC algorithm in three scenarios, the influence of number of target and radar is also taken into account. Simulation results demonstrate that RMSMI algorithm can improve the performance of interference suppression and convergence, and enhance the sensitivity of radar in both single target and multiple targets scenarios.

The remainder of this paper is organized as follows. Section 2 presents the received signal model for shared-spectrum multistatic radar. The RMSMI algorithm is developed in Section 3. Some implementation issues are discussed in the next section. Simulation results are shown and discussed in Section 5. Finally, conclusions are made in Section 6.

2. RECEIVED SIGNAL MODEL OF SHARED-SPECTRUM MULTISTATIC RADAR

In Fig. 1, K radars occupy the same spectrum simultaneously. It is obvious that each of the radars in the shared-spectrum system receives a superposition of its own reflected energy from the other radars operating in the area and noise. Note that only mainlobe to sidelobe path interference is included in the signal model, since it is implicitly assumed that the radars possess sufficient synchronization and/or exist in an appropriate spatial configuration so that direct path interference can be mitigated, and each transmitter possesses good control of its sidelobe.

It is known that the same processing is carried out at each radar with loss of generality; consequently the method is developed by considering only the ith radar. Assume all the K transmitting radars simultaneously emit the individual waveforms s_k, $k = 1 \ldots K$, sharing the same spectrum in close proximity, where $s_k = [s_k(0), s_k(1), \ldots s_k(N-1)]^T$.

The shared-spectrum multistatic radars occupy the same spectrum, and it is impossible to separate these signals in the frequency domain. These signals come from different directions, and the space filtering techniques (beamforming) can be used to suppress interference partially [17–20]. It is assumed that the antenna is just an L-length

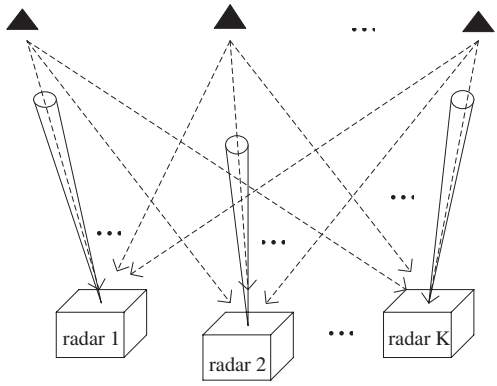

Figure 1. Configuration of shared-spectrum multistatic radar.

uniform linear array with digital beamforming capability. The spatial steering vector corresponding to the direction of arrival (DOA) of the reflected return signal resulting from the kth radar's mainbeam illumination which is incident at radar i is denoted as

$$r_k = [1, e^{j\theta_k}, \ldots, e^{j(L-1)\theta_k}]^T \tag{1}$$

where θ_k is the DOA of the return signal of the kth radar, the number of array elements is L, and $(\cdot)^T$ is the transpose operation.

The mth time sample on the lth antenna element of radar i can be expressed as

$$y_l(m) = \sum_{i=1}^{K} \mathrm{x}_i^T(m) e^{j(l-1)\theta_i} s_i + n_l(m) \tag{2}$$

where $m = 1, 2, \ldots, M$, the N-length vector $s_i = [s_i(0), s_i(1), \ldots, s_i(N-1)]^T$ states the sampled version of the transmitted waveform i. $\mathrm{x}_i(m) = [x_i(m), x_i(m-1), \ldots, x_i(m-N+1)]^T$ is N contiguous samples of the range profile, and n is additive noise. The vector $\tilde{y}(m) = [y_1(m), y_2(m), \ldots, y_L(m)]^T$ is the collection of received radar return signals on the L antenna elements for the mth time sample, upon which beamforming technology can be implemented.

Each antenna array element possesses its own receiving channel such as frequency down-conversion, A/D converter, I and Q formation, etc., thus digital beamforming capability is enabled. A separate normalized beamformer is described as

$$b_k = \frac{r_k}{L} \tag{3}$$

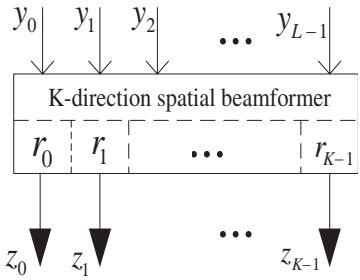

Figure 2. Processing flow of beamforming.

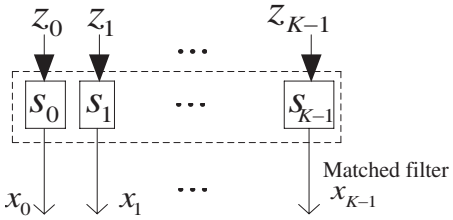

Figure 3. Pulse compression using the matched filter.

Figure 2 shows the processing diagram of beamforming, and the output of beamforming is expressed as

$$z_k(m) = b_k^H \tilde{y}(m) = \sum_{i=1}^{K} \gamma_{k,i} \mathrm{x}_i^T(m) s_i + u_k(m) \tag{4}$$

where $\gamma_{k,i} = \frac{r_k^H r_i}{L}$ is the normalized correlation between the kth and ith spatial beamformer. $(\cdot)^H$ is the complex-conjugate transpose (or Hermitian) operation, and $u_k(m) = \frac{r_k^H}{L}[n_1(m), n_2(m), \ldots, n_L(m)]^T$ denotes the noise vector after beamforming.

Range profiles of all radars can be obtained by using a bank of matched filters at the receiver, whose processing block diagram is illustrated in Fig. 3.

Standard matched filter is to convolve the received return signal with a complex-conjugated time-reversed copy of the transmitted waveform, so the range profile estimate is

$$\hat{x}_k(m) = s_k^H \tilde{z}_k(m) \tag{5}$$

where $\tilde{z}_k(m) = [z_k(m), z_k(m+1), \ldots, z_k(m+N-1)]^T$ is N contiguous temporal samples of the received signal corresponding to the kth

waveform after beamforming, which can be formed as

$$\tilde{z}_k(m) = \sum_{i=1}^{K} \gamma_{k,i} A_i^T(m) s_i + \tilde{u}_k(m) \tag{6}$$

where $A_i(m) = [\mathrm{x}_i(m), \mathrm{x}_i(m+1), \ldots, \mathrm{x}_i(m+N-1)]$ is a collection of sample-shifted snapshots of the range profile of the kth radar, and $\tilde{u}_k(m) = [u_k(m), u_k(m+1), \ldots, u_k(m+N-1)]^T$ is a N-length vector of noise after beamforming.

Range profile matrix $A_k(m)$ can be expressed as the summation of the diagonal matrix $A_{k,1}(m)$ and non-diagonal matrix $A_{k,2}(m)$ [21]

$$A_k(m) = A_{k,1}(m) + A_{k,2}(m) \tag{7}$$

where $A_{k,1}(m) = x_k(m) I_N$, and $x_k(m)$ is the range profile of the kth radar at the mth range cell. I_N is the $N \times N$ identity matrix.

Equation (6) is rewritten as

$$\begin{aligned} \tilde{z}_k(m) \;=\; & \gamma_{k,k} A_{k,1}^T(m) s_k + \gamma_{k,k} A_{k,2}^T(m) s_k \\ & + \sum\nolimits_{i \neq k} \gamma_{k,i} A_i^T(m) s_i + \tilde{u}_k(m) \end{aligned} \tag{8}$$

Equations (5) and (8) indicate that the result of the matched filter is the superposition of signal, range sidelobes, cross-correlation interference between waveforms and noise. The orthogonal transmitted waveforms are utilized to solve the mutual interference problem, but in practice it is impossible to guarantee a bank of waveforms orthogonal and waveform design cannot mitigate the mutual interference.

Range sidelobes generated by the matched filter may mask small nearby targets thereby inherently limiting radar detection sensitivity, and additive severe cross-correlation interference will further deteriorate the capability of the matched filter. The background is not only comprised of white noise in the presence of the interferences where the standard matched filter is not any longer optimal. Thus, the matched filter is not a proper choice for shared-spectrum multistatic radar, and a better filter is needed to suppress range sidelobe and interference from other radars as much as possible no matter what the transmitted waveforms are.

3. CO-FREQUENCY INTERFERENCE SUPPRESSION ALGORITHM BASED ON MAXSMIL

In order to suppress the range sidelobe, interference and noise effectively, a filter with weight vector $w_k(m)$ based on maximum signal minus interference level (MaxSMIL) is proposed, which makes

the result of signal power minus interference power maximum, hence interferences including sidelobes, co-frequency interference and noise are suppressed. RMSMI algorithm is to apply a bank of K RMSMI filters to take the place of a bank of K matched filters, and the general flow of pulse compression using RMSMI algorithm is illustrated in Fig. 4. The kth receiving RMSMI filter is obtained by minimizing the cost function

$$J(w_k(m)) = P_I - P_s \tag{9}$$

where P_I denotes the interference power after pulse compression and it is formed as

$$P_I = E\left[\left|w_k^H(m)\left(\gamma_{k,k}A_{k,2}^T(m)s_k + \sum\nolimits_{i\neq k}\gamma_{k,i}A_i^T(m)s_i + \tilde{u}_k(m)\right)\right|^2\right] \tag{10}$$

P_s denotes signal power after pulse compression, which is also the output of square-law detection and expressed as

$$P_s = E\left[\left|w_k^H(m)\gamma_{k,k}A_{k,1}^T(m)s_k\right|^2\right] \tag{11}$$

It is known that it can be also explained and expressed as given bellow

$$P_s = E\left[\left(w_k^H(m)\gamma_{k,k}A_{k,1}^T(m)s_k\right)\left(w_k^H(m)\gamma_{k,k}A_{k,1}^T(m)s_k\right)^H\right] \tag{12}$$

However, if the power is obtained by Equation (10), the cost function is minimized trivially if $w(m) = 0$. Ideally $w_k^H(m)\gamma_{k,k}A_{k,1}^T(m)s_k$ is equal to the desired signal $x_k(m)$, thus auto-correlation is altered by cross-correlation between desired signal and the output of the filter. So Equation (12) can be replaced by Equation (13) approximately

$$P_s \approx E\left[\left(w_k^H(m)\gamma_{k,k}A_{k,1}^T(m)s_k\right)(x_k(m))^*\right] \tag{13}$$

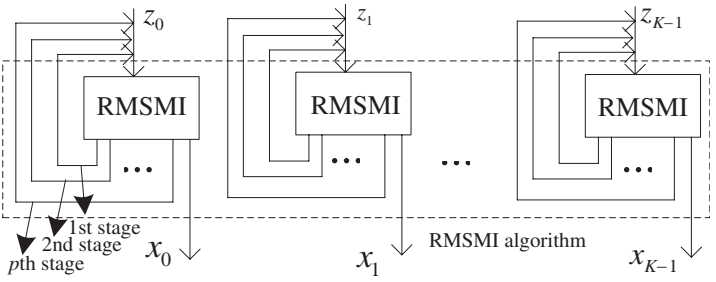

Figure 4. Pulse compression using RMSMI algorithm.

The cost function is minimized by taking the derivative of (9) with respect to $w_k(m)$, and then setting the result equal to zero. The RMSMI filter is formed as

$$w_k(m) = \gamma_{k,k}\rho_k(m)R_I^{-1}(m)s_k \tag{14}$$

where $\rho_k(m) = |x_k(m)|^2$ is the range cell power estimates, yet, it is impossible to know range profile in advance. The initial estimate of the range profile is obtained by using standard matched filtering. $R_I(m)$ is the interferences (including sidelobes, cross-correlation interference and noise) covariance matrix at the current range cell, and it is expressed as

$$R_I(m) = E\left[\left(\gamma_{k,k}A_{k,2}^T(m)s_k + \sum_{i\neq k}\gamma_{k,i}A_i^T(m)s_i + \tilde{u}_k(m)\right)\left(\gamma_{k,k}A_{k,2}^T(m)s_k + \sum_{i\neq k}\gamma_{k,i}A_i^T(m)s_i + \tilde{u}_k(m)\right)^H\right].$$

Assume that range profiles of all the radars at the same range cell are uncorrelated, and they are also uncorrelated with the noise. Therefore, interferences covariance matrix $R_I(m)$ is the summation of sidelobe covariance matrix $R_{side,k}(m)$, co-frequency interference covariance matrix $R_{I,k}(m)$ and noise covariance matrix $R_{n,k}(m)$

$$R_I(m) = R_{side,k}(m) + R_{I,k}(m) + R_{n,k}(m) \tag{15}$$

where $R_{side,k}(m) = E\left[\left(\gamma_{k,k}A_{k,2}^T(m)s_k\right)\left(\gamma_{k,k}A_{k,2}^T(m)s_k\right)^H\right]$,

$$R_{I.k}(m) = E\left\{\left(\sum_{i=1,i\neq k}^{K}\gamma_{k,i}A_i^T(m)s_i\right)\left(\sum_{i=1,i\neq k}^{K}\gamma_{k,i}A_i^T(m)s_i\right)^H\right\}$$

and $R_{n,k}(m) = E\left[\tilde{u}_k(m)\tilde{u}_k^H(m)\right]$.

Assume that neighboring impulse response terms are uncorrelated. Range sidelobe covariance matrix $R_{side,k}(m)$ and co-frequency interference (from other radars) covariance matrix $R_{I.k}(m)$ are respectively written as following

$$R_{side,k}(m)\,|\gamma_{k,k}|^2 \sum_{n=-N+1,n\neq 0}^{N-1}\rho_k(m+n)s_{k,n}s_{k,n}^H \tag{16}$$

$$R_{I,k}(m) = \sum_{i=1,i\neq k}^{K}\left(|\gamma_{k,i}|^2 \sum_{n=-N+1}^{N-1}\rho_i(m+n)s_{i,n}s_{i,n}^H\right) \tag{17}$$

where $s_{i,n}$ includes the elements of the ith transmitted waveform shifted by n samples, and the remainder is padded by zeros, e.g., $s_{i,3} = [0, 0, 0, s_i(0), s_i(1), \ldots, s_i(N-2)]^T$, when $n = 3$, and $s_{i,-3} = [s_i(3), \ldots, s_i(N-1), 0, 0, 0]^T$, when $n = -3$.

If noise is white Gaussian, then the noise covariance matrix $R_{n,k}(m)$ is depicted as

$$R_{n,k}(m) = \gamma_{k,k}\sigma^2 I_N \tag{18}$$

where σ^2 is the power of additive noise.

At the ith receiver, range profiles of all radars can be obtained by utilizing a bank of RMSMI filters, and the processing block diagram has been shown in Fig. 4. The operation flow chart of RMSMI algorithm is illustrated in Fig. 5, and the basic steps of the algorithm are described in Table 1.

Table 1. operation of RMSMI algorithm.

1 Gather the received samples $\tilde{y}(m) = [y_1(m), \ldots, y_L(m)]$, $m = M - 1 + 2p(N-1)$, where p is the number of the desired stages, and M is the length of processing window.
2 Collect the output of beamforming $\{z_k(-(p-1)(N-1)), \ldots, z_k(M-1+p(N-1))\}$ $z_k(m) = b_k^H \tilde{y}(m)$, $b_k = \frac{r_k}{L}$
3 Use the matched filter to estimate the initial impulse response coefficient estimates $\{x_{k,1}(-(p-1)(N-1)), \ldots, x_{k,1}(M-1-(p-1)(N-1))\}$. $x_{k,1}(m) = s_k^H \tilde{z}_k(m)$
4 Compute the power estimates $\rho_{k,p}(m) = \lvert x_{k,p}(m)\rvert^2$, then obtain the reiteration-stage filters $w_{k,p}(m)$. $w_{k.p}(m) = \gamma_{k,k}\rho_{k,p}(m)R_I^{-1}(m)s_k$
5 Obtain the range profile estimates $\{\hat{x}_{k,p}(-(p-2)(N-1)), \ldots, \hat{x}_{k,p}(M-1-(p-2)(N-1))\}$. $x_{k,p}(m) = w_{k,p}^H \tilde{z}_k(m)$, where $x_{k,p}(m)$ denotes the kth radar's range profile at the pth stage
6 Repeat steps 4 and 5, until the length of processing window is M.

4. IMPLEMENTATION ISSUES

In this section, the computational efficiency and robustness of RMSMI algorithm are discussed.

Robustness of RMSMI algorithm can be achieved by many methods, such as compressing the dynamic range of the range cell estimates, weighting and diagonal loading.

4.1. Computational Efficiency

To obtain RMSMI filter, it is necessary to find the inversion of the $N \times N$ interference covariance matrix, and $O(KN^3M)$ operations are required per stage. Large N or M causes computation burden. Therefore, measures should be taken to reduce computational complexity.

The employment of dimensionality reduction techniques can further reduce the computational cost. The $N \times N$ correlation matrix is segregated into Q blocks of $N_1 \times N_1$ matrices($N = QN_1$), and only $O(4N_1^2 + N)$ operations are needed for each range cell of each radar at each stage.

4.2. Numerical Stability

It is shown in Equation (14) that the matrix inverse estimation is required to obtain the weight, so the interference covariance matrix should be positive definite, and thus it is invertible. As the echo is random signal, the echo is affected by noise or clutter, and then the covariance matrix may become ill-conditioning. Therefore the weight may be not optimal any more.

One way to prevent matrix to be ill-conditioned is to compress the dynamic range of the power estimates of each range cell, which is achieved by replacing $\rho_k(m) = |x_k(m)|^2$ with $\hat{\rho}(m) = |\hat{x}(m)|^\alpha$ for $1 \leq \alpha \leq 2$. However, this step makes $\hat{\rho}(m)$ not the power of range cells any more, and this will cause matrix estimate error.

Inadequate estimate of the covariance will impact on the performance of RMSMI algorithm. The above manner is to realize compression of power dynamic by change the index of the equation $\hat{\rho}(m) = |\hat{x}(m)|^\alpha$ $(1 \leq \alpha \leq 2)$. Here a different measure is adopted, and the output of the RMSMI filter is divided by a constant more than one. $\rho_k(m) = |x_k(m)|^2$ is replaced by equation $\hat{\rho}(m) = |\hat{x}(m)/\lambda|^2$, for $\lambda > 1$. This operation is equal to adding a fixed constant to the diagonal of the covariance matrix, which, essentially, is the diagonal loading technique.

The diagonal loading is an effective method of suppressing the small eigenvalues and compensating for the estimate error of covariance matrix, which is to make the loaded covariance matrix $\bar{R}_I(m) = R_{side,k}(m) + R_{I,}k(m) + R_{n,k}(m) + \beta I$ in the place of interference covariance matrix $R_I(m) = R_{side,k}(m) + R_{I,}k(m) + R_{n,k}(m)$, and β is the diagonal loading factor, which is an integer multiple of 10 generally. The utilization of diagonal loading changes the matrix eigenvalue distribution and guarantees the matrix invertible. Therefore, the problem of matrix ill-conditioning can be solved by choosing an

appropriate diagonal loading factor.

5. SIMULATIONS

In this section, the effectiveness of the RMSMI algorithm for shared-spectrum multi-static radar will be demonstrated by three simulation experiments. Firstly, in Experiment 1, the interference suppression performance of RMSMI is compared with that of MAPC. Secondly, the interference suppression performance of RMSMI compared with that of MAPC is analyzed in multiple targets environment in Experiment 2. Finally, the influences of the number of radars working closely on the interference suppression performance of RMSMI are discussed.

In all experiments, assume that each of the radars is equipped with an 11-element uniform linear array, and the direction-of-arrival (DOA) of each radar echo is known. The transmission signal is linear frequency modulation (LFM) phase coding with code length $N = 30$, center frequency $f_0 = 60\,\text{MHz}$, bandwidth $B = 2\,\text{MHz}$ and sub-pulse width $\tau_c = 0.2\,\mu\text{s}$. The length M of processing window is chosen to be 100.

5.1. Experiment 1: Interference Suppression Performance of RMSMI and MAPC

In this experiment, assume that $K = 2$ radars work in the same frequency spectrum at the same time, irradiating one point target each in Gaussian background. The two targets are located at the 40th and 45th range cells, respectively. The DOA of the two radar echoes are 0° and 10° respectively.

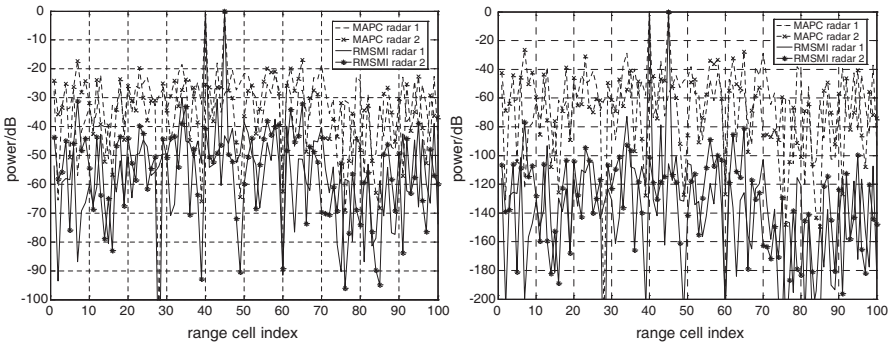

(a) Result after one iteration step (b) Result after two iteration steps

Figure 5. Results of pulse compression via RMSMI and MAPC algorithm.

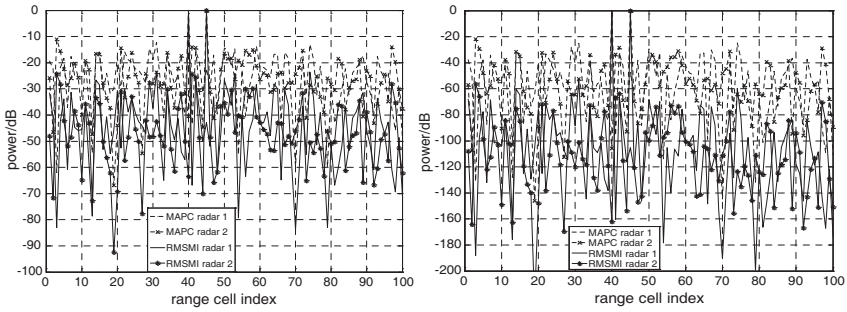

(a) Result after one iteration step (b) Result after two iteration steps

Figure 6. RResults of pulse compression via RMSMI and MAPC algorithm.

When the SNR at the receivers of radar antennas are both 0 dB, the results of pulse compression via RMSMI and MAPC algorithms are given in Fig. 5. Fig. 6 illustrates the results of RMSMI and MAPC when the SNR at the receivers of radar antennas are both −10 dB.

It is shown in Fig. 5(a) that, after one iteration step, the output SIR of the RMSMI filter reaches up to 37 dB while the output SIR of MAPC filter is only 27 dB. Thus, it can be inferred from the result that the RMSMI outperforms the MAPC in the capability of suppressing the interferences in the same environment since the output SIR of the RMSMI filter is improved by 10 dB more or less.

It is also shown in Fig. 5(b) that the interference suppression performance of MAPC after two iteration steps is similar to that of RMSMI after one iteration step, and the RMSMI has large performance gain over the MAPC after two iteration steps, which means that RMSMI can achieve a similar performance to MAPC through less iteration steps than MAPC. Thus, RMSMI has a faster convergence speed than MAPC.

In Fig. 6, it can be shown that when the SNR at the receivers of radar antennas are reduced to −10 dB, the output SIR of RMSMI filter after one and two iteration steps are 32 dB and 80 dB respectively, which are improved by 10 dB and 45 dB compared with those of MAPC respectively. The performance of MAPC after two iteration steps is similar to that of RMSMI after one iteration step, which demonstrates that RMSMI still has a faster convergence speed than MAPC in low SNR environment. Thus, it can be inferred that RMSMI still maintains its advantages over MAPC in suppressing the interferences, though the performance of both MAPC and RMSMI degrades when SNR is reduced.

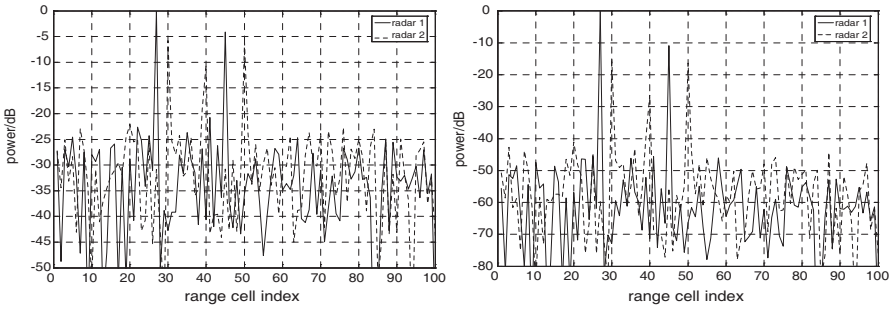

(a) Result of MAPC (b) Result of RMSMI

Figure 7. Results of pulse compression via RMSMI and MAPC algorithm.

5.2. Experiment 2: Interference Suppression Performance of RMSMI in Multiple Targets Environment

In Experiment 2, $K = 2$ radars working in the same spectrum at the same time in multiple targets environment in Gaussian background are considered too, with DOA of the two radar echoes 0° and 10°. Besides, assume that two point targets irradiated by radar1 are located at the 27th and 45th range cells in the processing window respectively. And SNR at receiver of antenna (ROA) are 0 dB and −4 dB respectively, while other three point targets irradiated by radar 2, whose SNR at ROA are −5 dB, −10 dB and −7 dB respectively, located at the 30th, 40th and 50th range cells. The results after one iteration step of RMSMI algorithm is shown in Fig. 7.

In Fig. 7, after one iteration step, the output SIR of the MAPC filter is 28 dB, while the RMSMI achieves 50 dB, which is 22 dB higher than that of MAPC. Therefore, the RMSMI still outperforms the MAPC in suppressing the interferences in multiple targets environment.

5.3. Experiment 3: The Influence of Number of Radars Working Closely on the Interference Suppression Performance of RMSMI

Assume that there are $K = 3$ radars working in the same frequency band at the same time in Gaussian background, with DOA of radar echoes are −10°, 0° and 10° respectively. Meanwhile, each radar irradiates only one point target. The three targets locate at the 40th, 45th and 50th range cells in processing window, respectively, and the SNR at ROA of them are both 0 dB. The results of MAPC and RMSMI

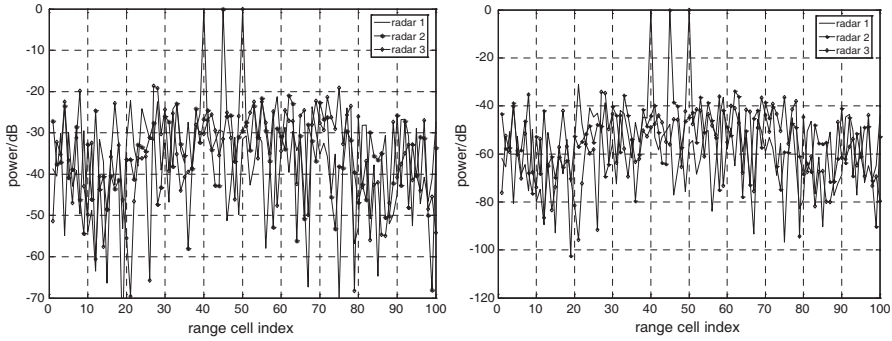

(a) Result of MAPC (b) Result of RMSMI

Figure 8. Results of pulse compression via RMSMI and MAPC algorithm.

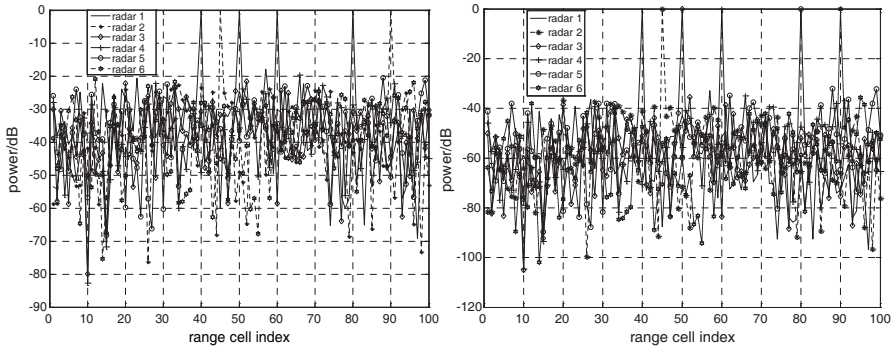

(a) Result of MAPC (b) Result of RMSMI

Figure 9. Results of pulse compression via RMSMI and MAPC algorithm.

algorithms are shown in Fig. 8.

Besides, let $K = 6$ radars work in the same spectrum at the same time also in Gaussian background, with DOA of radar echoes $-20°$, $-10°$, $0°$, $10°$, $20°$ and $30°$ respectively. Again, each of the radars irradiates only one point target. The six targets locate at the 40th, 45th, 50th, 60th, 80th and 90th range cells, respectively, and the SNR at ROA of them are both 0 dB. The results of MAPC and RMSMI algorithms are shown in Fig. 9.

Comparing Figs. 8, 9 and 5(a), it can be shown that after one iteration step, the output interference peak and the output SIR of the MAPC filter are -18 dB and 30 dB respectively while those of the RMSMI filter are -30 dB and 39 dB respectively. Thus, it

can be inferred that when the number of radars working closely increases, the RMSMI still maintaina its advantages over MAPC in suppressing the interferences. And RMSMI algorithm enables much more radars for the shared-spectrum application to work closely than the MAPC algorithm, while achieving the same interference suppression performance.

6. CONCLUSIONS

There is a severe co-frequency interference problem in shared-spectrum multi-static radar application. In order to suppress the co-frequency interferences effectively, the MSMIL-based adaptive pulse compression is proposed in this paper, which applies the adaptive compression to the echoes from multiple radars jointly and maximizes the result of the signal minus interferences, considering that the shared-spectrum multi-static radar echo is a sum of four components, including the target echo caused by mainlobe, target echo caused by range sidelobes, echo from other radars operating in the same spectrum and noise. The simulation results show that the range sidelobes and interferences from other radars working closely can be suppressed effectively via this algorithm. Compared with MAPC, the output SIR of the RMSMI filter is improved by 10 dB after one iteration step and more than 40 dB after two iteration steps. It also outperforms the MAPC in convergence speed. Moreover, RMSMI still maintains its advantages over MAPC in suppressing the interferences when SNR is reduced, though the performance of both MAPC and RMSMI degrades. The results also show that the numbers of targets and radars have little impact on the interference suppression performance of the RMSMI. Thus, the RMSMI enables more radars to share the same frequency band to work closely in different environments than the MAPC algorithm, achieving the same interference suppression performance, which can promote the development of the shared-spectrum multi-static radar to some extent.

REFERENCES

1. Isnard, J., "Frequency band sharing: Utopia or reality? Towards specification of operational scenarios," *IEEE Aerospace and Electronic Systems Magazine*, Vol. 17, No. 5, 4–9, 2002.
2. Richard, E., A. Kwaku, and D. George, "Federal communications commission report of the spectrum policy task force," http://www.fcc.gov/sptf/files/SEWGFinalReport_1.pdf, Nov. 2002.

3. Shamsan, Z. A., A. M. Al-Hetar, and T. B. A. Rahman, "Spectrum sharing studies of IMT-Advanced and FWA services under different clutter loss and channel bandwidths effecets," *Progress In Electromagnetics Research*, PIER 87, 331–344, 2008.
4. Krieger, G., H. Fiedler, and J. Mittermayer, "Analysis of multistatic configurations for spaceborne SAR interferometry," *IEE Proceedings Radar, Sonar and Navigation*, Vol. 150, No. 3, 87–96, 2003.
5. Zhang, M. Y. and X. G. Wang, *Radar System*, 2nd edition, 370–390, Publishing House of Electronics Industry, Beijing, 2006.
6. He, Z. S., C. L. Han, and B. Liu, "MIMO radar and its technical characteristic analyses," *Chinese of Journal Electronics*, Vol. 33, No. B12, 2441–2445, 2007.
7. Wang, G. H. and Y. L. Lu, "Sparse frequency waveform design for MIMO radar," *Progress In Electromagnetics Research B*, Vol. 20, 190–32, 2010.
8. Al-Kamali, F. S., M. I. Dessouky, B. M. Sallam, and F. E. A. El-Samie, "Frequency domain interference cancellation for single carrier cyclic prefix CDMA systems," *Progress In Electromagnetics Research B*, Vol. 3, 255–269, 2008.
9. Al-Kamali, F. S., M. I. Dessouky, B. M. Sallam, and F. E. A. El-Samie, "Frequency domain interference cancellation for single carrier cyclic prefix CDMA systems," *Progress In Electromagnetics Research B*, Vol. 3, 255–269, 2008.
10. Blunt, S. D. and G. Karl, "Aspects of multistatic adaptive pulse compression," *Proceedings of the IEEE International Radar Conference*, 104–108, Arlington, VA, May 9–12, 2005.
11. Karl, G. and S. D. Blunt, "A novel approach to shared-spectrum multisattic radar," *Proceedings of the IEEE International Radar Conference*, 437–443, Verna, NY, Apr. 24–27, 2006.
12. Karl, G., S. K. Aaron, and S. D. Blunt, "Combined multistatic adaptive pulse compression and adaptive beamforming for shared-spectrum radar," *IEEE Journal of Selected Topics in Signal Processing*, Vol. 1, No. 1, 137–145, 2007.
13. Blunt, S. D. and G. Karl, "A generalized formulation for adaptive pulse compression of multistatic radar," *4th IEEE Workshop on Sensor Array and Multichannel Processing*, 349–353, Waltham, MA, Jul. 12–14, 2006.
14. Blunt, S. D. and G. Karl, "Multistatic adaptive pulse compression," *IEEE Transaction on Aerospace and Electronic Systems*, Vol. 42, No. 3, 891–903, 2006.

15. Blunt, S. D. and G. Karl, "Hybrid adaptive receive processing for multistatic radar," *2nd IEEE International Workshop on Computational Advance in Multi-Sensor Adaptive Processing*, 5–8, Dec. 12–14, 2007.
16. Blunt, S. D., W Dower, and G. Karl, "Hybrid interference suppression for multistatic radar," *IET Radar, Sonar and Navigation*, Vol. 2, No. 5, 323–333, 2008.
17. Guney, K. and S. Basbug, "Interference suppression of linear antenna arrays by amplitude-only control using a bacterial foraging algorithm," *Progress In Electromagnetics Research*, PIER 79, 475–497, 2008.
18. Mouhamadou, M., P. Armand, P. Vaudon, and M. Rammal, "Interference supression of the linear antenna arrays controlled by phase with use of SQP algorithm," *Progress In Electromagnetics Research*, PIER 59, 251–265, 2006.
19. Castaldi, G., V. Galdi, and G. Gerini, "Evaluation of a neural-network-based adaptive beamforming scheme with magnitude-only constraints," *Progress In Electromagnetics Research B*, Vol. 11, 1–14, 2009.
20. Mahmoud, K. R., M., El-Adawy, and S. M. M., Ibrahem, "Performance of circular Yagi-Uda arrays foe beamforming applications using particle swarm optimization algorithm," *Journal of Electromagnetics Waves and Applications*, Vol. 22, 353–364, 2008.
21. Zhang, J. D., H. Q. Wang, and X. H. Zhu, "Adaptive pulse compression via MSN criteria," *Journal of Electronic and Information Technology*, Vol. 3, No. 4, 790–793, 2009.